STRUCTURAL BEHAVIOR OF CFRP RETROFITTING OF DEFICIENT STEEL TUBULAR T JOINT UNDER AXIAL LOADING

S. M. Zahurul Islam[*1]K. M. Redwanul Hasan Rana[2], F. Ahmed Adittya[3], I.Uddin Munna[4], M. Golam Amin[5]

[1]Head, Architecture Dept. & Professor, Dept. of Civil Engineering, RUET, Bangladesh
e-mail: zahurul90@gmail.com
[2&3] Under Graduate Student, Department of Civil Engineering, RUET, Bangladesh
[4&5] Under Graduate Student, Department of Civil Engineering, BAUET, Natore, Bangladesh

***Corresponding Author**

ABSTRACT

Steel tubular members are extensively used due to their lightweight and excellent load-carrying capacity in the form of frames, trusses, girders and vierendeel. T-joints are commonly used in tubular member joint by vertical member with horizontal chord, mid span, trusses and beam-column in frame. The load bearing capacity as well as structural performance depends on the strength of its connections. Steel tubular T-joints usually are vulnerable due to local buckling as well as instability of the web under axial compressive loading. The failure of T-joint of steel structure may lead to the progressive damage of the whole structure. Carbon Fiber Reinforced Polymer (CFRP) is one of the most promising composite materials for strengthening of steel tubular structures. CFRP Strengthening of T-joints can be considered to overcome ductility, strength, inadequate performance of the steel structures T-joint. The objective of this study is to investigate on structural performance of CFRP retrofitting of deficient steel tubular T-joint under axial loading. An extensive test programs have been conducted to strengthen the steel tubular joints by CFRP composites under axial loading. Twelve steel tubular joint including reference specimens were tested in this research with varying the influence parameters.Load-deflection behavior, the failure loads, the failure modes have been presented due to axial loading. The load carrying capacity improved significantly and varied 19.63%-63.82% for different strengthening technique. ABAQUS software has been used to simulate CFRP strengthening steel tubular joints of the test results. Material and Geometrical non-linearity (*NLGEOM) was considered for the analysis. Excellent agreement has been attained between the FE simulations and the tested results. Developed finite element model is verified with test result. Hence, it can be demonstrated that the improving structural performance can be achieved for steel tubular T-joints by CFRP composites strengthening under axial loading.

Keywords: *Axial loading, CFRP, Steel tubular T-joint, Strengthening, Structural behaviour*

1. INTRODUCTION

Steel tubular members are increasingly being used in the building, bridges, offshore platform, stadium, airport hangar and different long-span structures due to their cost effectiveness, light weight and aesthetic appearance. Steel joint is weakest part of the steel structures. Most of the steel structures were collapse due to failure of joints. Tubular members T-joint can be damaged due to seismic action, over loading corrosion, accidental collision, overloading. To ensure the structural integrity of these integral constructions, the development of robust and reliable joints is essential. In a tubular structure, T-joint play a significant and vital role for load transferring elements as a crucial structural component. The collapse of T-joint of steel structure may lead to the progressive damage of the whole structure. Over the past few decades, various retrofitting methods have been deployed to address this problem (Rajak et al., 2020).Welded tubular structures have gained significant traction in civil engineering since the 1950s, following the resolution of issues related to manufacturing, end preparation, and welding processes (Wardenier et al., 2002). Previous many studieshave conducted research on steel and stainless T-joint without any strengthening by the authors Ran (2008) and Zhao and Tong (2011).Three researchers have investigated–on T-joint compressive behaviour strengthening by vertical inner plate and collar plate by the authors Chang et. al. (2018) and Deng et. al. (2019),Aguilera, and Fam, (2013). External steel plate cutting and attaching is general and conventional method of repairing and strengthening steel tubular structures (Zhao and Zhang, 2007). However, retrofitting using steel plates has some drawbacks. The heavy weight of steel plate is difficult to handle and install. The erection time is relatively long by using steel plate retrofitting. It was reported that cutting and attaching plate retrofitting method is laborious, bulky, tedious, corrosion and fatigue prone. Therefore, there is a need to find alternative solutions. The method of retrofitting using CFRP would avoid these problems.

CFRP composite materials have gained popularity as a way to strengthen steel structures in recent years. Because of its outstanding properties, including as high tensile strength, a high elastic modulus, low weight, and adaptability in application to constructions of varied forms, CFRP composites are the preferred choice for retrofitting hollow steel sections. CFRP retrofitting techniques have garnered growing interest for enhancing the performance of not only concrete structures but also steel structures.It has been demonstrated that bonding CFRP sheets or plates to steel plates, beams, or welded plate-to-plate joints effectively improves their performance.Recently, different CFRP retrofittingtechnique have been applied on tubular member-joint to increase axial compressive load carrying capability. In literature review, tubular member K and X joint have been investigated byXu et al., (2020), Mohamed et al.(2022), Fu, et al., (2016).Research was conducted on external stiffening rings boost structural resilience and stability in response to axial stresses (Osman et al., 2023). Ultimate load carrying capacity of the cracked T/Y tube joint could be effectively restored by wrapping FRP (CFRP) sheets around the joints (Lesani et al., 2014). External stiffening rings can be improved the axial compressive strength of circular hollow section (CHS) T-joints. This study examined that stress concentration factors (SCF) in FRP-reinforced tubular T-joints. They provided unique insights into tubular T-joint performance and behaviour when strengthened with FRP materials under various loading circumstances (Sadat et al., 2019).Hosseini et al. (2020a, 2020b),

A research conducted on behaviour of circular hollow section (CHS) gap K-joints reinforced with CFRP by Fu et al., (2016) . They showed that 3D simulation of K-joints with CFRP done by ABAQUS and verified it. This study constructed and verified a three-dimensional computational model using experimental data K-joint composed of CFRP. Finite element modelling used to evaluate the effects of various parameters on CFRP strengthening efficiency, measured by the stress concentration factor reduction coefficient (Xu et al., 2020). A macro-code in ANSYS FEM software modelled base panel damage and core shear failure. The study also found that sandwich panel core material affected joint failure stress (Khalili & Ghaznavi, 2011). Strengthening methods for joints are

often believed to prevent premature debonding, even though many researchers have observed instances of debonding occurring with this approach.Deng et al. (2020) had investigated on CFRP strengthening T-joint by numerical for compressive behavior. There is a clear gap among researchers on the effectiveness of retrofitting and strengthening deficient steel tubular T-joint under axial loading by CFRP materials. However, fewresearchers have been conducted on the application of CFRP materials for strengthening and retrofitting of deficient steel tubular T-joint under axial loading. Therefore, it is an innovative approach to study on strengthening and retrofitting of deficient steel tubular T-joint under axial loading by CFRP.

The purpose of this research is to investigate on structural behavior of CFRP retrofitting of deficient steel tubular T-joint under axial loading. A series of test programs have been conducted to retrofit the steel T tubular joints by CFRP composites under axial loading. Twelve steel tubular joint including reference specimens were tested in this research with varying the influence parameters. Load-deflection behavior, the failure loads, the failure modes have been presented due to axial loading. The load carrying capacity improved significantly.Numerical software (ABAQUS) has been used to simulate CFRP retrofitting steel tubularT-joints of the test results. Developed finite element model is verified with test result.Good agreement has been attained between the FE simulations and the tested results. The improving structural performance can be achieved for steel tubular T-joints by CFRP composites strengthening under axial loading.

2. EXPERIMENTAL PROGRAMS

2.1 Material Properties

Tubular metallic structures are widely employed due to their lightweight and high load-carrying capacity. This study involved the preparation of test specimens using three different materials: mild steel (MS), CFRP wrap, and adhesive, as depicted in Figure 1. The effectiveness of externally bonded strengthening primarily relies on the characteristics of the metal surface, adhesive, and CFRP materials. Key mechanical properties for strengthening structures include the effective bond strength, elastic modulus, and elongation of the adhesive. CFRP material is a composite consisting of fibers embedded in a resin matrix, with epoxy resin being the most commonly used for CFRP. In this research, CFRP fabrics of the Kor-CFW450 type were utilized, featuring a fiber strength of 4900 MPa, fiber stiffness of 230 GPa, a weight of 450 g/m^2, and a fabric thickness of 0.255 mm. Primer and saturant were used with densities of 1.14 gm/cm^3 and 1.8 gm/cm^3, pot life durations of 30 minutes and 1 hour 30 minutes, and tensile strengths of 1350 MPa and 4875 MPa, along with moduli of elasticity of 99.37 GPa and 238.00 GPa, respectively. The adhesive used in this research is Kor-CPA 10 Base Resin, and its associated hardener has a tensile strength of 49.8 MPa and a shear strength of 29 MPa, with a pot life of 70 minutes. The mild steel coupon specimens had a thickness of 1.3 mmand 2.3 mm were prepared from tubular sections in accordance with American and Australian standards. The mild steel tubular sections had a tensile yield stress of 390 MPa, an ultimate stress of 450 MPa, and an initial Young's modulus of 198.6 GPa.These mechanical propertiesof mild steel were obtained from the previous research conducted by Islam et al., (2023).

Figure 1: Primer, Adhesive and CFRP

2.2 Test Specimens and Specimen Preparation

A series of tests have been conducted to strengthen the steel tubular T-joints by CFRP composites under axial loading.In this study, square and circular tubular two types of sections were used to prepareT-joint. SHS steel had a dimension of 51mm x 51mm. The length of horizontal and vertical of SHS steel were 305mm and 254 mm respectively. Also, the thickness of the material was 1.30mm. On the other hand, CHS steel had diameter 75 mm and the horizontal and vertical dimension of 254mm x 254mm, with thickness 2.30mm.Joining the tubular steel bars to form T-joints as shown in Figure 2.

Figure 2: Welding steel tubular section to build T-joints

The steel joints were intentionally cut transversely to create a weakened member, as depicted in Figure 3. This cutting process was performed using a grinding machine with a diamond-tipped blade. Each joint was initially treated with a primer, with a waiting period of 30 minutes. Subsequently, epoxy was applied to the joints, followed by the wrapping of CFRP around them. Schematic view T-joint is shown in Figure 4. Epoxy mixing then attached CFRP to T-joint surface is illustrated in Figure 5. The steel joint specimens were left undisturbed for a week to allow the epoxy to fully cure and reach its maximum strength as shown in Figure 6.

Figure 3: Cracking to make deficient T-joints by grinding machine

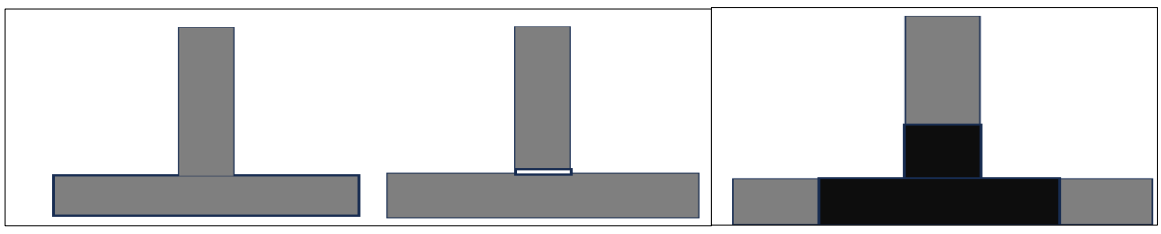

Figure 4: Schematic view of uncracked, cracked and CFRP strengthen T-joint

Figure 6: Circular and square tubular section T-joint specimen without and with CFRP

2.3 Instrumentations and Loading Procedure

Schematic view and lab test setup of the tubular steel joints is shown in Figure7. To measure joint deflection, a vertical linear variable differential transducer (LVDT) was employed. Additionally, threeLVDT were affixed to the centre of the joints on different sides. The testing of all joints for deformation was carried out using a MATEST compression testmachine. The experimental research incorporated two control methods: load control and displacement control. Initially, load control was applied, with the load being restricted to the yield strength of the joint. Subsequently, displacement control was implemented, with a focus on monitoring and controlling displacement until the failure of joint.

Figure 7: Schematic view of test setup and test arrangement of the tubular steel section T-joints.

3. TEST RESULTS AND DISCUSSIONS

An extensive test program has been conducted on CFRP retrofitting of deficient steel tubular T-joint under axial loading. Twelve circular and square mild steel tubular member T-jointspecimensincluding reference and initially pre-cracked T-joint was tested in this research to verify the influence of two parameters such as light cutting and deep deficient. The specimens were labelled as $CS_1C_0F_0$,$CS_1C_0F_1$,$CS_1LC_1F_0$,$CS_1LC_1F_1$,$CS_1DC_1F_0$,$CS_1DC_1F_1$,$SS_1C_0F_0$, $SS_1C_0F_1$, $SS_1LC_1F_0$, $SS_1LC_1F_1$, $SS_1DC_1F_0$,$SS_1DC_1F_1$. Where, CSindicates circular sections, SS indicates square sections, C_o indicates reference jointno pre-crack and F_o indicate no CFRP, C_1 indicateone layer crack; $F_{1,}$ indicates one-layer CFRP retrofitted. The mild steel T-joint tests were conducted by MATEST compressive testing machine. Four linear variable differential transducer (LVDT) was used for determining the deflection of the test specimen. The loadings were obtained from the test machine as it is built with the help of computerized function.The failure loads, failure modes and the load-deformation behavior of reference joint and CFRP retrofittedjointwere observed in this research. The failure modes of unstrengthen and CFRP strengthen T-joint are shown in Fig. 8.The failure patterns of square T-joints subjected to compressive loading are depicted. The failure of the CFRP-strengthened joint sample is illustrated in Figure 8(a-d), and it predominantly exhibits a debonding type of failure. Notably, no rupturing of the CFRP sheets is evident, underscoring the high tensile strength of CFRP. Once the debonding of the CFRP occurs from the steel surface, the sample experiences a decline in peak load and a subsequent loss of strength. The debonding of the CFRP appears to be attributed to issues with the steel surface rather than epoxy failure. A deep cut pattern is showcased in $SS_1DC_1F_1$, where CFRP is present only on the tension face in Figure 8(d). Despite initially achieving an ultimate load of 28.46kN, this load-bearing capacity diminishes as the load increases further.

(a) (b) (c) (d)

Figure 8: Failure mode of deficient tubularT-joints(a) $SS_1LC_1F_1$ (b) $SS_1DC_1F_1$

The failure patterns of circular T-joints subjected to compressive loading are also presented in Figure 8. The failure of the $CS_1LC_1F_1$ strengthened joint is visualized in Figure 8(a).Local bucking failure is observed in unstrengthen tubular short column specimen. The presence of shear strips has not only increased the load-carrying capacity but also altered the failure pattern, confining the crack within the two shear strips. A glimpse of the deep cut in the $CS_1DC_1F_1$ joint sample is provided in Figure 8(b). Notably, no rupture of the CFRP is discernible, and some parts of the concrete surface are clearly visible, confirming that the failure did not occur in the CFRP or the epoxy.Improving structural performance in terms of load ultimate load carrying capacity is shown inTable 1. The load carrying capacity improved significantly and varied 19.63%-63.82% for different strengthening technique.

Table 1: Load caring capacity enhancement for CFRP Retrofitting of Circular& square tubular T-joints

Specimen Designation		Sl No.	Specimen Designation	Ultimate Load (kN)	Enhanced Load Capacity (%)	Type of Failure
Mild Steel Tubular Section T-Joint	Circular	1	$CS_1C_0F_0$	11.74	---	Local buckling & bulging
		2	$CS_1C_0F_1$	15.24	19.63	CFRP cracks and yielding
		3	$CS_1LC_1F_0$	8.76	----	Local buckling & concave
		4	$CS_1LC_1F_1$	13.25	51.26	CFRP cracks and yielding
		5	$CS_1DC_1F_0$	07.19	----	Local buckling & concave
		6	$CS_1DC_1F_0$	11.78	63.82	CFRP cracks and yielding
	Square	7	$SS_1C_0F_0$	25.75	----	Local buckling & concave
		8	$SS_1C_0F_1$	35.90	39.42	CFRP cracks and yielding
		9	$SS_1LC_1F_0$	19.72	-----	Local buckling & concave
		10	$SS_1LC_1F_1$	28.46	44.32	CFRP cracks and yielding
		11	$SS_1DC_1F_0$	17.6	-----	Local buckling & concave
		12	$SS_1DC_1F_1$	26.65	51.42	CFRP cracks and yielding

The load versus deflection curves for the tested square T-joints is shown in Figure 9. The $SS_1C_0F_0$ specimen exhibited a maximum peak load value of 25.75 kN at an 8 mm displacement. Subsequent to reaching this peak load, the specimen experienced a loss of stiffness, and the load began to decrease, indicating the failure of the sample. This decrease resulted from the transfer of tensile strain through the combined action of epoxy and steel.Due to the higher stiffness of CFRP, the $SS_1C_0F_1$ specimen displayed a peak load value of 35.90 kN, which is approximately one and a half times the strength of the $SS_1C_0F_0$. In comparison to $SS_1LC_1F_0$, the load and joint deflection curves for the T-section strengthened with CFRP, but with the joint cut, showed significant improvements. Specifically, sample $SS_1LC_1F_1$, featuring CFRP sheets solely on the tension face, increased its strength from 19.72 kN to 28.46 kN. This increase in joint strength was notable. Moreover, when the joints were deep cut

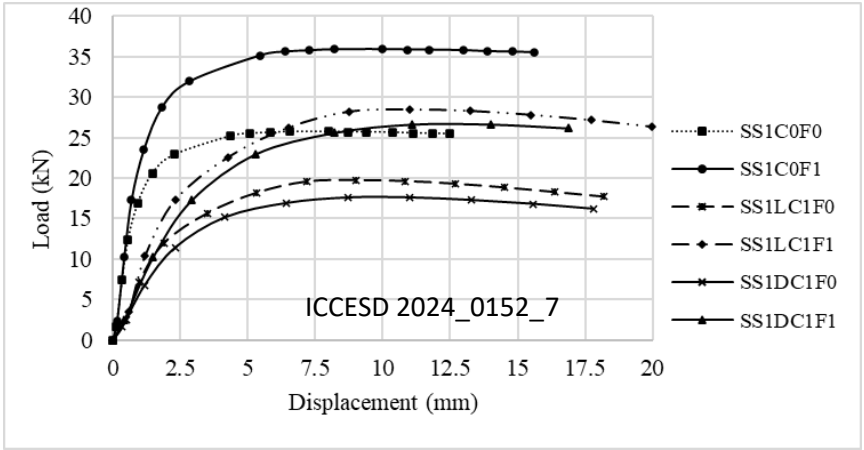

on the sides, it enhanced the load-carrying capacity from 17.6 kN ($SS_1DC_1F_0$) to 26.65 kN ($SS_1DC_1F_1$), which is roughly 1.5 times the strength of the joints illustrates in Figure 9. These findings emphasize the crucial role of CFRP on the tensile face in retrofitting the T-joints.

Figure 9: Load-displacement curve for square tubular joints

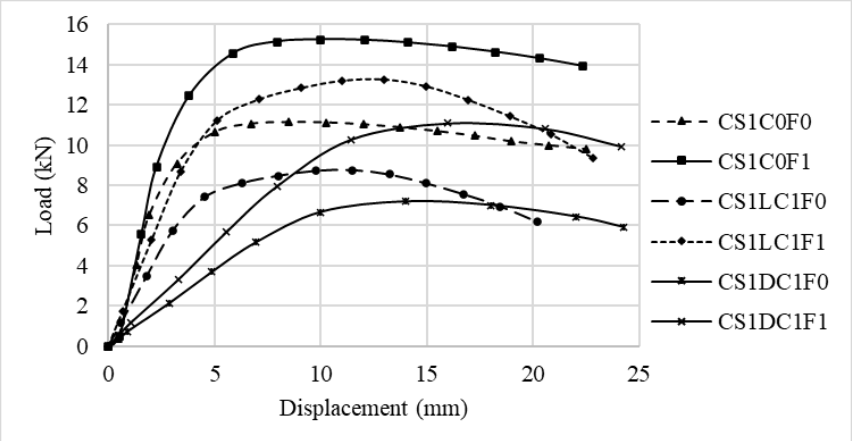

Figure 10: Load-displacement curve for circular tubular joints

The load and deflection curves for circular T-joints that were subjected to compressive loading testing as shown in Figure 10. These curves represent both cut and wrapped CFRP joint specimens. For the $CS_1C_0F_0$ samples, which had no cuts and featured CFRP sheets, they exhibited a maximum load of 11.14 kN at a joint deflection of 8.5 mm. In contrast, the $CS_1C_1F_1$ specimens, where CFRP was used for reinforcement, showed a behavior similar to square T-joints, with a higher peak load of 15.24 kN. $CS_1LC_1F_0$ and $CS_1LC_1F_1$, featuring cuts in the joints and CFRP reinforcement, displayed peak load values of 8.76 kN and 13.25 kN, at displacements of 11.5 mm and 13 mm, respectively. The peak strength of $CS_1LC_1F_1$ was approximately 1.5 times that of the $CS_1LC_1F_0$ samples as shownin Figure 10 However, it's worth noting that the peak displacements were significantly smaller in the CFRP-strengthened steel joint samples, indicating their higher stiffness.

Based on experimental observation, it can be revealed that by increasing CFRP length and number of layers, load carrying capacity enhancement also is increased. Deformation is also increased due to CFRP retrofitting. The strength enhancement in terms of load carrying capacity significantly varied from 51.26-63.82% and 44.32-51.42%, for light and deep deficient retrofitted for circular and square T-joint, respectively. Failure load have increased due to CFRP retrofitting and local buckling shifted to yield failure. Therefore, better performance can be attained by CFRP strengthening of deficient metaltubular short columns with appropriate technique.

4. NUMERICAL INVESTIGATIONS

4.1 Finite Element Model Development Strategies

In the development of Finite Element (FE) model, it is essential to address the representation of five key components: Bearing plate, steel, CFRP sheets, adhesive and interface between steel- adhesive, adhesive and CFRP sheets. Everyelementwas accurately modelled to capture their distinctive properties. To simulate bearing plate, a common approach was involved the utilization of discrete rigid 3D solid elements element, designated as C3D8 in ABAQUS. In the case of modelling steel the preferred choice is often shell elements, denoted as S4R in ABAQUS. CFRP sheet were simulate by also shell element. These elements were well-suited for materials with orthotropic properties.To model the interface between FRP and steel, tie contact pair elements are employed. One such element

is the cohesive element were assigned for adhesive, designated as COH3D8 in ABAQUS. This cohesive element takes the form of a 3D eight-node zero-thickness linear interface element, with the capability to simulate bonded interfaces and potential delamination between them (Islam et.al., 2018). The use of these elements necessitates the precise alignment of nodes on both surfaces. This element tracks normal stresses and slippage at these interfaces, which may arise from bending or shear actions. The separation between two adjacent surfaces is represented by increasing the displacement between the nodes within the interface element itself.

4.2 Interaction, boundary condition and Mesh of Finite Element

The interaction module constraint makes use of the degrees of freedom between the mode areas, and

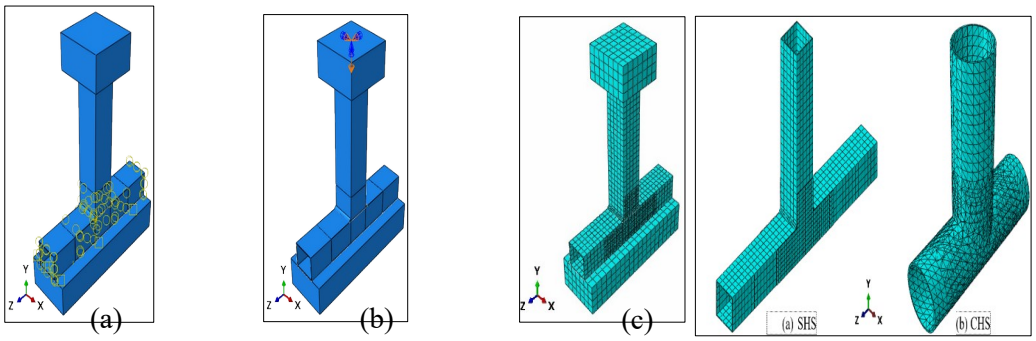

Figure 11: Finite element model (a) interaction (b) load applied (c) meshing of T-joint

the numerical model can be changed by repeating and suppressing the constraints. The master surface and slave surface were defined creating constraints and were picked manually. Tie constraint is used between the layers of steel and welded portion, steel and epoxy resin, epoxy resin and CFRP as in Figure 11(a).The selected BC type, "ENCASTRE," effectively repairs the specimen at this end. Specifically, it was deployed zeros for all displacement and rotation degrees of freedom (U1 = U2 = U3 = UR1 = UR2 = UR3 = 0) except Y direction to allow displacement. Theload was applied to the upper end of the specimen, as shown in Figure 11(b). Various mesh size was tried to get mesh convergence.The mesh size for various components was selected based on their dimensions and significance. The CFRP component, the steel joint, and the load-bearing part were meshed with finer elements of sizes 6.5mm, 10mm, and 15mm, respectively as in Figure 11(c).

4.3 Mode of Failure of Simulation of Finite Element Analysis

Comparison of test and finite element model failure mode of square and circular deficient tubular joints is shown in Figure 12. Good agreement has been attained between the failure mode of FE simulations and the tested failure mode. HenceStress distribution and failure of CFRP retrofitted damaged T-joint is shown in Figure 13. The farthest border of the FRP is represented by Point A in this photo the laminate's centre is perfectly represented by Point B, and Point C is situated halfway between points A and B. Point A's (the outer edge of the FRP laminate) stress levels are clearly low, as seen by the blue hue, which signifies low stress. The stress in the FRP laminate changes to an intermediate level as we approach the centre of the laminate (Point C). This intermediate level is indicated by the red hue, which denotes a higher stress level than Point A. Lastly, at Point B, the FRP laminate's stress is significantly greener than it is at points A and C. The full load is transferred through the FRP laminate at point B, where the green colour indicates a heightened stress magnitude.

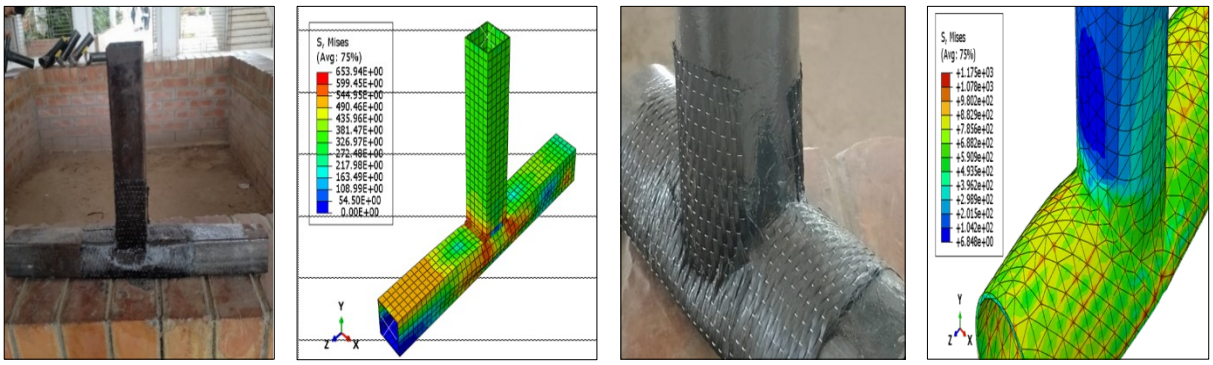

Figure 12: Comparison of Test and finite element model failure mode of squarecircular deficient tubular joints

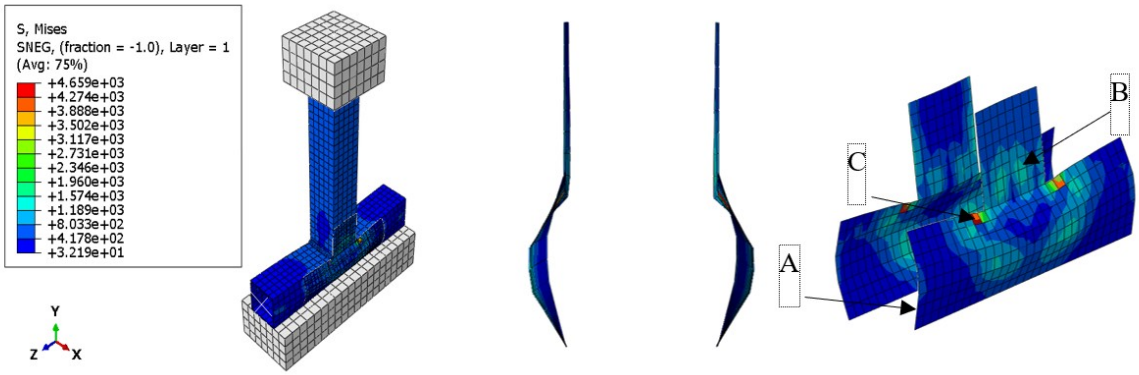

Figure 13: Stress distribution of FEMmodel square deficient tubular T-joints

4.4 Comparison between the Experimental and FEA Analysis

Developed finite element model is verified with lab test result. The load-displacement curves for square and circular T-joints in both test and FE-based numerical simulations as shown in Figure 14 and 15 respectively. The control sample exhibited a peak load of 25.75 kN in the experiment and 28.5 kN in the numerical simulation, as depicted in Figure 14(a). The numerical simulation closely aligned with the experimental results, indicating good agreement in load-displacement values predicted by ABAQUS, especially before the samples reached their failure point. However, there was a noticeable variation in the post-peak behaviour of the sample, possibly due to ABAQUS limitations in modelling the post-peak cracking behaviour of steelT-joints, influenced by the damage model used for steel failure prediction.The load-displacement behaviour of a T-jointspecimen wrapped with CFRP is shown for both numerical and experimental results in Figure 14(b).

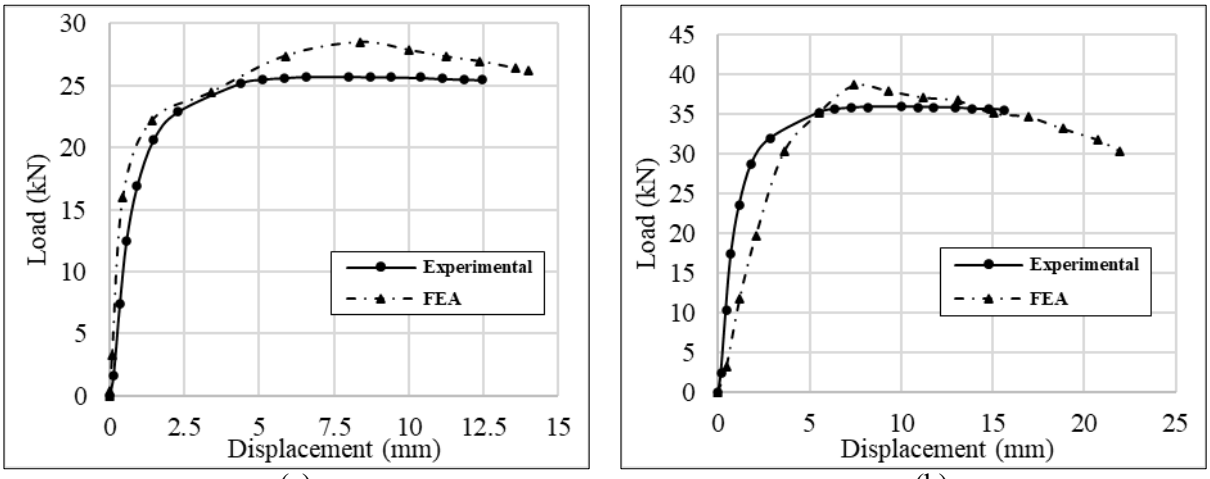

Figure 14: Comparison of load-displacement curve between deficient tubular joints for square joints (a) no cut without CFRP (b) no cut with CFRP

The peak load determined by the numerical simulation was slightly higher than the experimental peak load. This difference may be attributed to the favourable surface behaviour exhibited by the steel, epoxy, and FRP interface in the tested joint sample. Variations in steel surface quality and non-uniform epoxy application can significantly affect the experimental peak values compared to numerically predicted loads. Both experimental and numerical peak loads were observed at nearly the same displacement level of around 20-25 mm. A similar trend was observed for deep cut with CFRP specimen until a displacement level of 25-30 mm, after which the numerical model exhibited significant stiffness increases, resulting in a smaller peak load, as shown in Figure 15(a). The load-displacement curves for circular T-joints also provided similar pattern of results. In the case of a sample without cuts but with CFRP, the numerical peak load value predicted by ABAQUS (16.02 kN) closely matched the experimental peak load value (15.24 kN), as shown in Figure 15(b). Similar trends were observed in the numerical simulations of light cut with CFRP-strengthened samples as 15(c). However, when considering the post-peak behaviour or residual deformations, the numerical results did not align with the experimental values in Figure 15(d). This discrepancy can be attributed to the inelastic behaviour of cut T-joint sections, especially when the cuts are sufficiently deep, and steel surfaces are no longer in contact. The numerical results were generally similar to the experimental findings, they tended to show slightly lower values for slip, with an average difference of 0.46%. Additionally, the ultimate load exhibited a somewhat lower peak, with an average difference of 3.37%. Therefore,good agreement has been attained between FE simulations and the tested load-displacement curve. This FEM model can be extended to parametric study for larger and different section of full-scaleT-jointas well as different steel joint.

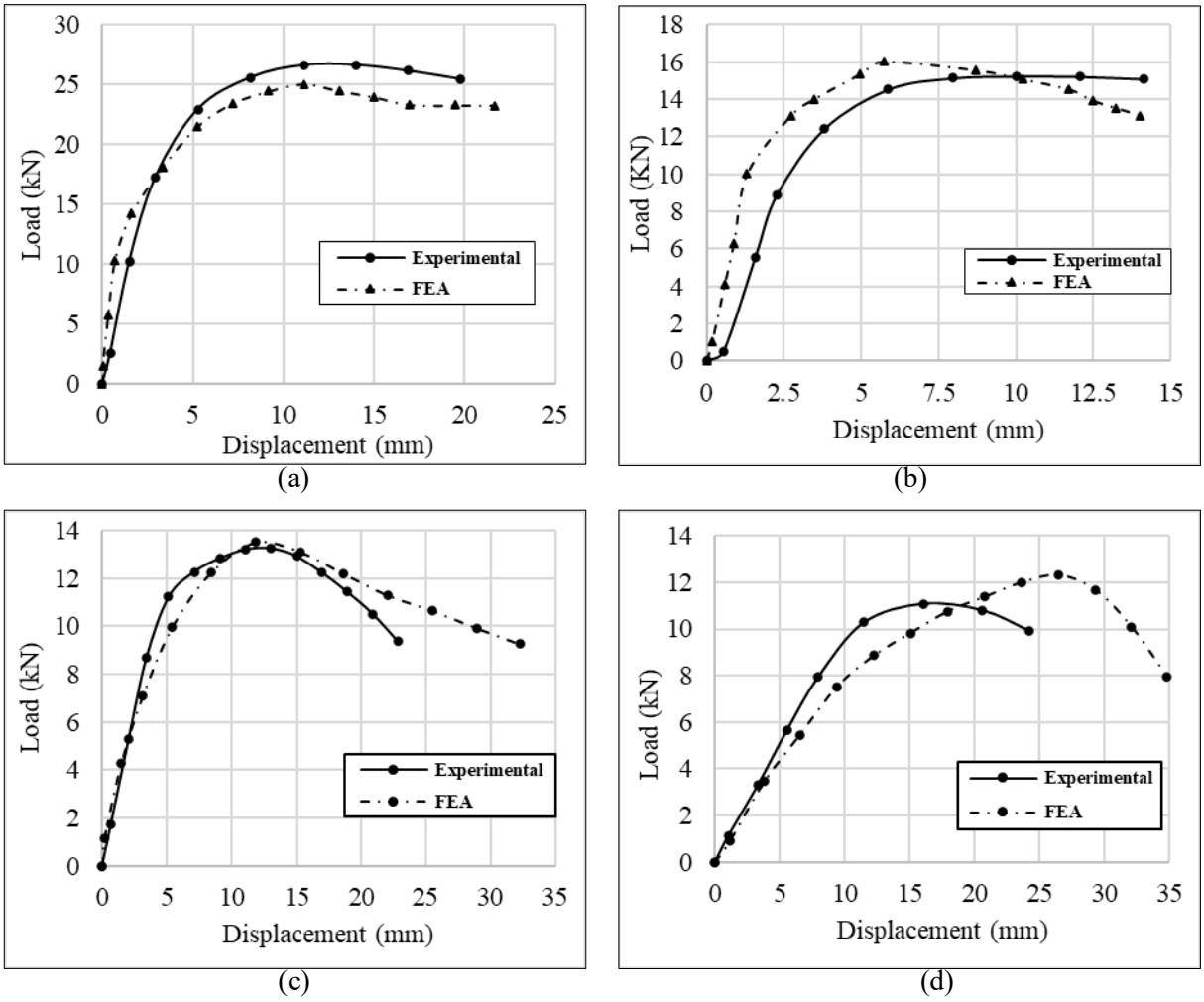

Figure 15: comparison of load-displacement curve between test and FEA of deficient square tubular section t-joints (a) deep cut with CFRP; and for circular joints (b) no cut with CFRP (c) light cut with CFRP (d) deep cut withCFRP.

5. CONCLUSIONS

An experimental and numerical model was developed to assess the performance of strength tests for CFRP-to-steel T-joints with various degrees of deficiency, specifically, different types of cuts. The results of this study yielded the following findings:

- In experiments involving circular-shaped T-joints, the application of CFRP led to an increase in load-bearing capacity as well as ductility. The load carrying capacity increased by 19.63%, 51,26%, and 63.82% for specimens without cuts, those with light cuts, and those with deep cuts, respectively.
- In the case of square-shaped T-joints, a similar trend was observed. The use of CFRP resulted in load-bearing capacity improvements of nearly 40%, 45%, and 52% for specimens without cuts, those with light cuts, and those with deep cuts, respectively.
- The inclusion of cohesive contact behavior in the numerical model, which simulated the surface interaction between steel and CFRP sheets, produced results that closely paralleled the experimental curves.
- Good agreement has been attained between FE simulations (ABAQUS) and the tested results.

- It can be concluded that the improving structural performance can be achieved for steel tubular T-joints by CFRP composites retrofitting under axial loading with effective technique.

ACKNOWLEDGEMENT

The financial support (Project No.: DRE/7/RUET/640(53)/Pro/2023-2024/02) provided by the University Grants Commission of Bangladesh is gratefully acknowledged. The authors are grateful to the Nutech Construction Chemicals Company Limited, Dhaka and Department of Civil Engineering, RUET, Rajshahi.

REFERENCES

Aguilera, J. Fam, A. (2013). Retrofitting tubular steel T-joints subjected to axial compression in chord and brace members using bonded FRP plates or through-wall steel bolts, *Engineering Structures*, Volume 48, March 2013, 602-610.

Chang, H., Xia, J., Guo, Z., Hou, C., Din, W., & Qin, F. (2018). Experimental study on the axial compressive strength of vertical inner plate reinforced square hollow section T-joints. *Engineering Structures*, 172, 131–140.

DengP., GuoJ., Liu,Y. and Zhongying W. Z.(2019). Compressive Behavior of Damaged Tubular T-joints Retrofitted with Collar Plate, KSCE *Journal of Civil Engineering*, DOI 10.1007/s12205-019-0276-y.

Deng P., Yang B., Chen X. Liu Y. (2020). Experimental and numerical investigations of the compressive behavior of carbon fiber-reinforced polymer strengthened tubular steel T-joints,*Front. Struct. Civ. Eng*.https://doi.org/10.1007/s11709-020-0663-y

Fu, Y., Tong, L., He, L., & Zhao, X.-L. (2016). Experimental and numerical investigation on behavior of CFRP-Strengthened Circular Hollow section gap k-joints. *Thin-Walled Structures*, 102, 80–97.

Hosseini A. Sadat, Bahaari M.R., and Lesani M. SCF distribution in FRP-strengthened tubular T-joints under brace axial loading,*Scientia Iranica A* (2020a) 27(3), 1113,1129

Hosseinia A. S., Bahaaria,M. R., Lesani M. (2020b). Experimental and parametric studies of SCFs in FRP strengthened tubular T-joints under axially loaded brace.*Engineering Structures,*213, 110548

Islam, S. M., Ahamed, M., Zaman, Md. T., Islam, Md. M., Abrar, T. S., Himel, O. F., Sattar, Md. M., & Ahmed, T. U. (2022). "Investigation on CFRP-strengthened aluminum, mild steel and stainless-steel tubular members under impact loading." 6th international conference on civil engineering for sustainable development (ICCESD 2022).

Islam S. M. Zahurul, Ben Young (2018). Design of CFRP-Strengthened Aluminium Tubular Sections subjected to Web Crippling,*Journal of Thin-walled Structures*, Elsevier Science, Volume 124, March 2018, Pages 605-621

Khalili, S. M. R., & Ghaznavi, A. (2011). Numerical Analysis of adhesively bonded T-joints with structural sandwiches and study of design parameters. *International Journal of Adhesion and Adhesives,* 31(5), 347–356.

Lesani, M., Bahaari, M. R., & Shokrieh, M. M. (2014). Experimental investigation of FRP-strengthened tubular T-joints under axial compressive loads,*Construction and Building Materials*, 53, 243–252.

Mohamed H.S. et al. Stress concentration factors of CFRP-reinforced tubular K-joints via Zero Point Structural Stress,*Approach.Marine Structures*, 84 (2022) 103239

Osman, A., Gerguis, P., & Gaawan, S. (2023). Performance of externally reinforced chs X-joints subjected to axial loads. *Journal of Engineering and Applied Science*, 70(1). https://doi.org/10.1186/s44147-023-00210-y

Rajak D. K., Wagh P. H, Kumar A., Sanjay M. R.,,Siengchin S., Khan A., Asiri A. M., Naresh, K., Velmurugan, R., Gupta, N.K. (2022). Impact of fiber reinforced polymer composites on structural joints of tubular sections: A review, *Thin-Walled Structures*, 180, 1-13.

Ran F. (2008) Design of cold-formed stainless steel tubular joints. PhD Thesis, Department of Civil Engineering, The University of Hong Kong. Hong Kong, China.

Sadat Hosseini, A., Bahaari, M. R., & Lesani, M. (2019). Stress concentration factors in FRP-strengthened offshore steel tubular T-joints under various brace loadings. *Structures*, 20, 779–793. https://doi.org/10.1016/j.istruc.2019.07.004

Wardenier, J., Packer, J. A., Zhao, X. L., & Van der Vegte, G. J. (2002). Hollow sections in structural applications. Rotterdam, The Netherlands: Bouwen met staal.

Xu, G., Tong, L., Zhao, X.-L., Zhou, H., & Xu, F. (2020). Numerical analysis and formulae for SCF reduction coefficients of CFRP-strengthened CHS gap K-joints. *Engineering Structures*, 210, 110369. https://doi.org/10.1016/j.engstruct.2020.110369

Zhao, X. L. and Zhang, L. (2007). "State-of-the-art review on FRP strengthened steel structures." *Engineering Structures*, 29(8), 1808-1823.

Zhao1, X.L, and Tong,L.W. (2011). New Development in Steel Tubular Joints, (2011), *Advances in Structural Engineering,* 14 (4), 699-715.